

Purdue University Purdue e-Pubs

Department of Electrical and Computer
Engineering Faculty Publications

Department of Electrical and Computer
Engineering

1989

Effective minority-carrier hole confinement of Si-doped, n+-n GaAs homojunction barriers

H. L. Chuang
Purdue University

M. E. Klausmeier-Brown
Purdue University

Michael R. Melloch
Purdue University, melloch@purdue.edu

Mark S. Lundstrom
Purdue University, lundstro@purdue.edu

Follow this and additional works at: <https://docs.lib.purdue.edu/ecepubs>

 Part of the [Electrical and Computer Engineering Commons](#)

Chuang, H. L.; Klausmeier-Brown, M. E.; Melloch, Michael R.; and Lundstrom, Mark S., "Effective minority-carrier hole confinement of Si-doped, n+-n GaAs homojunction barriers" (1989). *Department of Electrical and Computer Engineering Faculty Publications*. Paper 84.
<http://dx.doi.org/10.1063/1.343868>

This document has been made available through Purdue e-Pubs, a service of the Purdue University Libraries. Please contact epubs@purdue.edu for additional information.

Effective minority-carrier hole confinement of Si-doped, n^+ -n GaAs homojunction barriers

H. L. Chuang, M. E. Klausmeier-Brown, M. R. Melloch, and M. S. Lundstrom

Citation: **66**, (1989); doi: 10.1063/1.343868

View online: <http://dx.doi.org/10.1063/1.343868>

View Table of Contents: <http://aip.scitation.org/toc/jap/66/1>

Published by the [American Institute of Physics](#)

Effective minority-carrier hole confinement of Si-doped, n^+-n GaAs homojunction barriers

H. L. Chuang, M. E. Kiasmeier-Brown, M. R. Melloch, and M. S. Lundstrom
School of Electrical Engineering, Purdue University, West Lafayette, Indiana 47907

(Received 6 February 1989; accepted for publication 7 March 1989)

The electrical performance of Si-doped n^+-n GaAs homojunction barriers grown by molecular-beam epitaxy (MBE) is characterized and analyzed. We employed a successive etch technique to study hole injection currents in GaAs n^+-n-p^+ solar cells. The results of the analysis show that minority-carrier holes in our MBE-grown material have a mobility of 293 $\text{cm}^2/\text{V s}$ for an n -type Si-doping level of $1.5 \times 10^{16} \text{ cm}^{-3}$ at 300 K. The interface recombination velocity for these homojunction barriers is estimated to be less than $1 \times 10^3 \text{ cm/s}$, and it appears to be comparable to that recently observed for Si-doped n^+-n GaAs homojunction barriers grown by metalorganic chemical vapor deposition. We present evidence that these n^+-n GaAs homojunctions, unlike p^+-p GaAs homojunctions, are almost as effective as AlGaAs heterojunctions in minority-carrier confinement, and that their electrical performance is not degraded by heavy doping effects.

I. INTRODUCTION

High-efficiency GaAs solar cells routinely employ high-low junctions for confining minority carriers.^{1,2} Depending on whether the cell is n^+-p or p^+-n , the high-low junction (also known as back-surface field or minority-carrier mirror) is either a p^+-p or n^+-n homojunction. Recent work has demonstrated that p^+-p GaAs homojunctions are not effective minority-carrier mirrors.³ The poor confinement was attributed to strong effective band-gap narrowing in $p^+-\text{GaAs}$ which lowers the confining potential for minority carriers. In this paper we examine n^+-n GaAs homojunction barriers and demonstrate that, in contrast with p^+-p homojunction barriers, they are effective minority-carrier mirrors. The interface recombination velocity of these homojunctions is quite comparable to that of heterojunction barriers, and is sufficient for most solar cell applications. These results suggest that the strong effective band-gap narrowing which occurs in $p^+-\text{GaAs}$ is absent in $n^+-\text{GaAs}$.

Both the experiment conducted and the techniques employed are similar to those we recently described for p^+-p GaAs homojunctions.^{3,4} The experiment itself and the results obtained are briefly described in Sec. II. These results are analyzed in Sec. III in order to deduce the interface recombination velocity of the n^+-n gallium arsenide homojunctions. In Sec. IV we compare the interface recombination velocity deduced from electrical measurements with that computed theoretically. Finally, our conclusions are summarized in Sec. V.

II. EXPERIMENTAL TECHNIQUE AND RESULTS

The epitaxial layer structure for the solar cells used in this study is shown in Fig. 1. The films were grown in a Varian GEN II molecular-beam epitaxy (MBE) system. The starting substrate was cleaved from a (100)-oriented, p -type GaAs wafer, and the thicknesses of the epitaxial layers were determined by counting oscillations in the intensity of the reflection high-energy electron diffraction pattern. Silicon was used as the n -type dopant and beryllium as the p -

type dopant. Solar cells of dimension $0.1 \times 0.1 \text{ cm}^2$ were defined by photolithography and subsequent wet etching. The ohmic contact to the $n^+-\text{GaAs}$ cap layer was a AuGe/Ni/Ti/Au metal finger pattern fabricated using a low-temperature annealing process. The back contact metal was indium. The doping density of the n layer was measured as $1.5 \times 10^{16} \text{ cm}^{-3}$ by capacitance versus voltage profiling. Doping densities of the other layers were determined from the calibrated temperatures of the dopant ovens.

A successive etch technique was used to characterize the hole injection current.⁴ The metal grid pattern was protected with photoresist, and the exposed semiconductor was removed in a series of short etches. Each etch was 20 s long in a solution of $[6\text{H}_2\text{SO}_4:3\text{H}_2\text{O}_2:400\text{H}_2\text{O}]$ at 27 °C and removed 250 Å of material, as measured by step profiling. After each etch, the short-circuit current I_{sc} under constant illumination through a 546-nm narrow-band filter, and the forward-biased dark I - V characteristics were measured. All I - V measurements were performed with a Hewlett-Packard 4145A semiconductor parameter analyzer at 23.3 °C.

The dark I - V characteristic measured after each etch step was analyzed to extract the $n = 1$ saturation current density J_{01} ; the results are plotted in Fig. 2. J_{01} did not increase until the $n^+-\text{GaAs}$ barrier layer was completely removed. It is important to note that J_{01} remained fairly constant as the $n^+-\text{AlGaAs}$ heteroface and $n^+-\text{GaAs}$ barrier layers were being etched away. This result clearly demonstrates that the homojunction barrier is as effective as the heterojunction barrier in minority-carrier hole confinement. This is in sharp contrast with the results that we obtained from a similar experiment for Be-doped, p^+-p GaAs homojunction barriers grown by MBE.³ In that experiment, we employed p^+-p-n^+ solar cells of similar structure and comparable doping densities (see Fig. 3), and found that J_{01} increased significantly as the $p^+-\text{GaAs}$ barrier layer was being etched away (see Fig. 4).

The fact that the n^+-n GaAs homojunction appears to be a good minority-carrier mirror is further substantiated by the short-circuit current I_{sc} versus etch depth plot, as shown

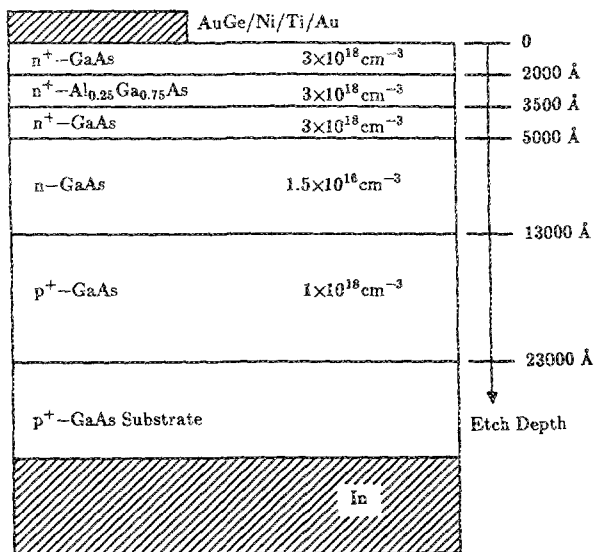


FIG. 1. Epitaxial layer structure of the solar cells used in this experiment.

in Fig. 5. I_{sc} rose as the n^+ -GaAs cap layer was etched away and more photons passed through the AlGaAs layer, generating electron-hole pairs. I_{sc} rose at a faster rate after the AlGaAs layer was exposed, due to the different absorption coefficients of the AlGaAs and GaAs layers. When the AlGaAs layer was completely removed, I_{sc} plummeted because some carriers generated in the n^+ -GaAs barrier layer recombined at the front surface. I_{sc} again rose as the barrier layer was etched away and more carriers were generated behind the barrier where they were collected. When the n^+ -GaAs barrier layer was completely removed, I_{sc} plummeted to the lowest point due to the very high surface recombination velocity of the bare GaAs surface. As the n -GaAs layer was thinned and more carriers were generated closer to the n - p^+ junction, I_{sc} rose gradually. Notice that the two peaks

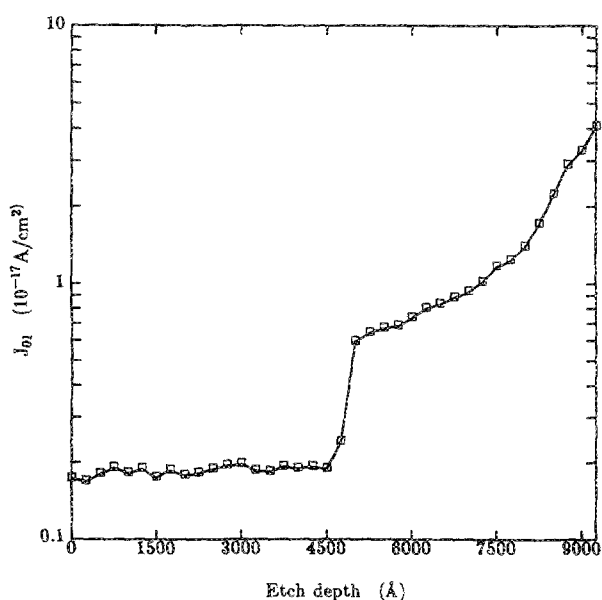


FIG. 2. J_{01} measured in this experiment.

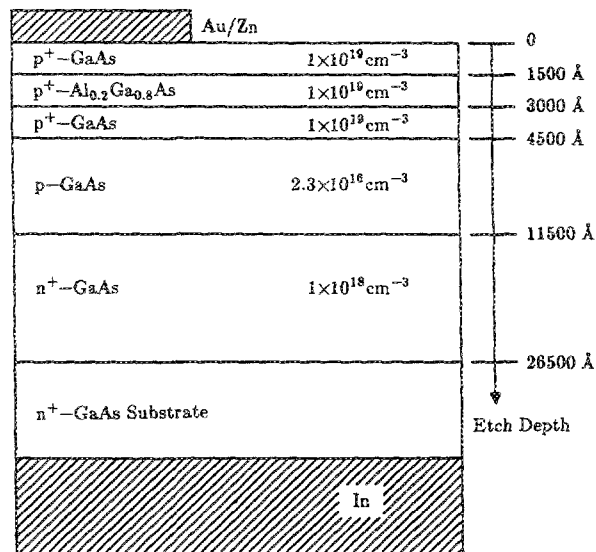


FIG. 3. Epitaxial layer structure of the solar cells used in a similar experiment for Be-doped, p^+ - p GaAs homojunction barriers (see Ref. 3).

that occurred just before the complete removal of the heterojunction and homojunction barriers have nearly equal heights. This indicates that these two different types of barriers are almost equally effective.

III. ANALYSIS

In an n - p^+ GaAs diode, the component of J_{01} due to hole injection in the n -GaAs is given by

$$J_{01p} = \frac{qn_0^2}{N_D} \left(\frac{S_n + (D_p/L_p) \tanh(W_n/L_p)}{1 + S_n(L_p/D_p) \tanh(W_n/L_p)} \right), \quad (1)$$

where D_p and L_p are the minority-carrier hole diffusion coefficient and length, respectively, n_0 is the intrinsic carrier

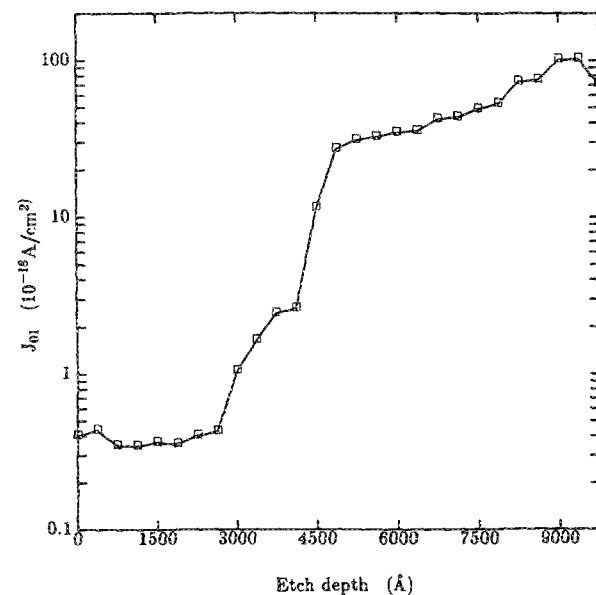


FIG. 4. J_{01} measured in a similar experiment for Be-doped, p^+ - p GaAs homojunction barriers (see Ref. 3).

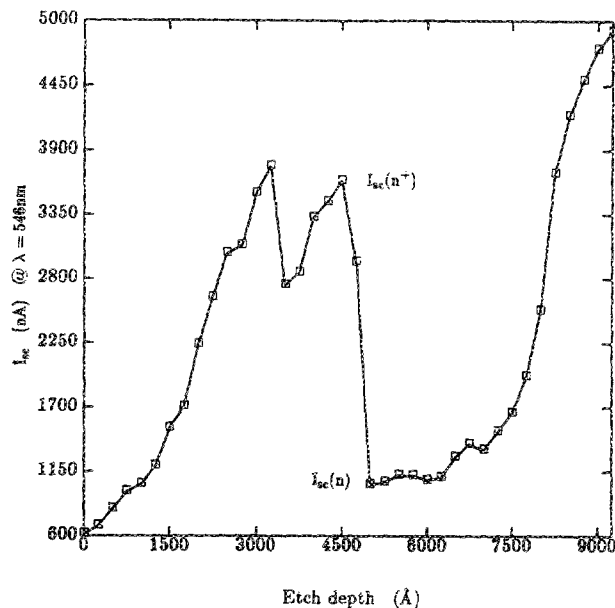


FIG. 5. Short-circuit current measured under constant illumination through a 546-nm narrow-band filter.

concentration of lightly doped GaAs, W_n is the width, and S_n is the recombination velocity at the surface of the lightly doped n layer. If the n layer is thin ($W_n \ll L_p$) and the surface is unpassivated ($S_n \gg W_n/\tau_p$), then Eq. (1) can be simplified as

$$J_{01p} = \frac{qn_0^2 D_p}{N_D W_n} \frac{S_n}{S_n + D_p/W_n}. \quad (2)$$

Equation (2) should describe the hole injection current after the n^+ -GaAs cap, the n^+ -AlGaAs, and the n^+ -GaAs barrier layers have been removed. Before these layers are completely removed, S_n is low and J_{01} is dominated by electron injection into the p^+ -GaAs. This implies that J_{01p} of Eq. (2) is the difference between the J_{01} measured after the top three layers were removed and that measured initially, which we denote by J_{01e} .

The width of the n -GaAs layer varied with the etch time according to $W_n(t) = W_{n0} - Rt$, where W_{n0} is the undepleted width of the n layer at $t = 0$, and R is the etch rate. Equation (2) can then be rearranged as

$$J_{01p}^{-1} = (J_{01} - J_{01e})^{-1} = \left(\frac{N_D W_{n0}}{qn_0^2 D_p} + \frac{N_D}{qn_0^2 S_n} \right) - \left(\frac{N_D R}{qn_0^2 D_p} \right) t. \quad (3)$$

Figure 6 shows that a plot of J_{01p}^{-1} versus etch time was linear with a slope of $N_D R / qn_0^2 D_p$, from which the product, $n_0^2 D_p$ at 23.3 °C, was determined to be $1.82 \times 10^{13} \text{ cm}^{-4} \text{ s}^{-1}$. From the intercept, the surface recombination velocity, S_n , was deduced to be $1.1 \times 10^7 \text{ cm/s}$, which agrees well with the value expected for a bare GaAs surface.^{3,5}

From the measured $n_0^2 D_p$ product and the data of Blakemore⁶ for n_0 (which is 1.55×10^6 at 23.3 °C), a minority-carrier hole diffusion coefficient of $D_p = 7.6 \text{ cm}^2/\text{s}$ was deduced. This value corresponds to a minority-carrier hole

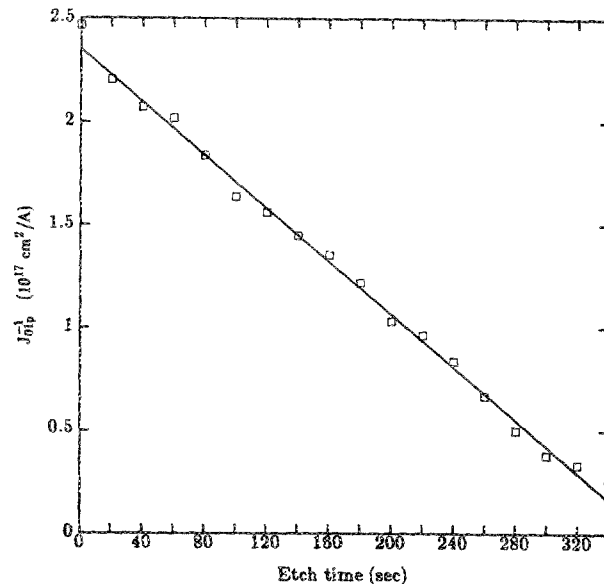


FIG. 6. J_{01p}^{-1} vs etch time was linear with a slope of $N_D R / qn_0^2 D_p$, from which D_p and μ_p were deduced.

mobility of $293 \text{ cm}^2/\text{V s}$ at 300 K. Venkatsubramanian *et al.*⁷ have reported somewhat lower minority-carrier hole diffusion coefficients in n -GaAs material grown by metalorganic chemical vapor deposition (MOCVD). They measured diffusion coefficients of 6.5 and $2.5 \text{ cm}^2/\text{s}$ for doping densities of 3×10^{15} and $4 \times 10^{16} \text{ cm}^{-3}$, respectively.

The interface recombination velocity S_{n^+-n} of the n^+-n GaAs homojunction barrier can be estimated from the ratio $I_{sc}(n^+)/I_{sc}(n)$, where $I_{sc}(n^+)$ and $I_{sc}(n)$ represent the short-circuit currents measured just before and after the complete removal of the n^+ -GaAs barrier layer, respectively. Using a theoretical expression for short-circuit current derived by Sze⁸ with the S_n and D_p measured here, we calculated the ratio $I_{sc}(n^+)/I_{sc}(n)$ for a series of minority-carrier hole lifetimes and interface recombination velocities. The results, $I_{sc}(n^+)/I_{sc}(n)$ vs S_{n^+-n} , are shown in Fig. 7. The actual $I_{sc}(n^+)/I_{sc}(n)$ measured from the short-circuit current plot (Fig. 5) is 3.51. From Fig. 7, an upper limit for the interface recombination velocity of $1 \times 10^3 \text{ cm/s}$ and a lower limit for the minority-carrier hole lifetime of 10 ns can be estimated. These estimates imply that the minority-carrier hole diffusion length L_p is greater than $2.75 \mu\text{m}$. The low interface recombination velocity obtained here is at least 60 times lower than that of Be-doped, p^+-p GaAs homojunction barriers grown by MBE.³ This clearly indicates that the n^+-n barrier is superior to the p^+-p barrier in minority-carrier confinement.

These results can be used to check our assumptions that were made in the derivations of Eqs. (2) and (3). Since the minority-carrier hole diffusion length L_p is greater than $2.75 \mu\text{m}$ and the hole lifetime τ_p is more than 10 ns, and the surface recombination velocity S_n of the bare GaAs surface is $1.1 \times 10^7 \text{ cm/s}$, therefore the assumptions ($W_n \ll L_p$) and ($S_n \gg W_n/\tau_p$) used in Eq. (2) are valid. Since ($W_n \ll L_p$) and S_{n^+-n} is comparable to W_n/τ_p , Eq. (1) can be simplified as

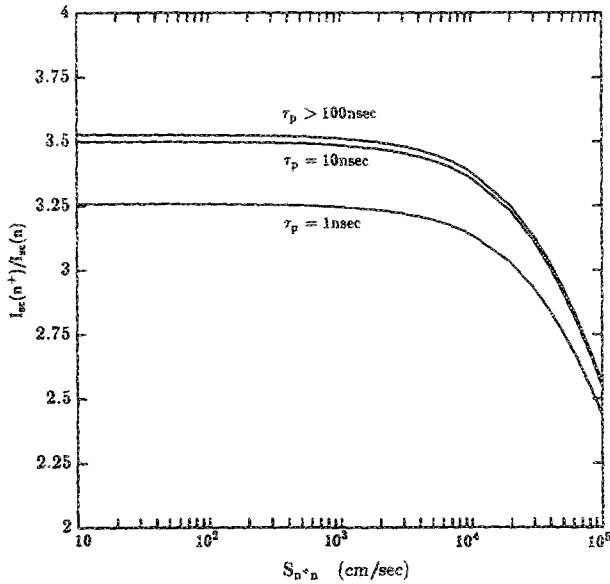


FIG. 7. Ratio of short-circuit currents calculated for a series of minority-carrier hole lifetimes and interface recombination velocities. $I_{sc}(n^+)$ and $I_{sc}(n)$ represent the short-circuit currents just before and after the complete removal of the n^+ -GaAs barrier layer, respectively.

$$J_{01p} = \frac{qn_D^2}{N_D} \frac{S_{n^+-n} + W_n/\tau_p}{1 + (W_n/D_p)S_{n^+-n}} \quad (4)$$

By assuming an upper limit of 1×10^3 cm/s for S_{n^+-n} and a lower limit of 10 ns for τ_p in Eq. (4), we estimated that the upper limit of J_{01p} only contributes less than 8% of the initial J_{01} measured before the lightly doped n layer is exposed. This implies that the initial J_{01} is dominated by electron injection current J_{01e} and that the assumption used in Eq. (3) is valid.

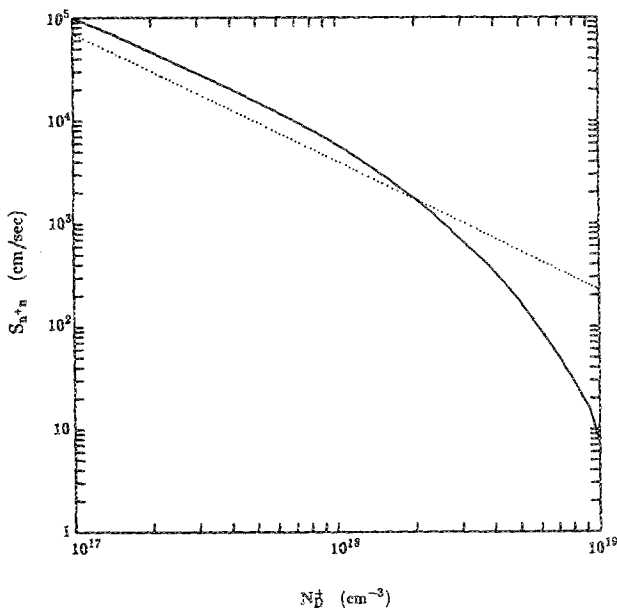


FIG. 8. Theoretical estimates of S_{n^+-n} with and without heavy doping effects vs a range of heavy doping concentrations, N_D^+ , represented by solid and dotted lines, respectively.

IV. DISCUSSION

The theoretical interface recombination velocity of the n^+-n GaAs homojunction⁹ can be computed from

$$S_{n^+-n} = \frac{D_p^+ N_D^- n_{ie}^2}{L_p^+ N_D^+ n_D^2} \coth\left(\frac{W_n^+}{L_p^+}\right), \quad (5)$$

where the $-$ and the $+$ superscripts refer to the lightly and heavily doped sides of the junction, respectively, n_D is the intrinsic carrier concentration of lightly doped GaAs, and n_{ie} is the effective intrinsic carrier concentration of the heavily doped GaAs. Since the n^+ -GaAs barrier layer is only 0.15 μm thick, $W_n^+ \ll L_p^+$, so Eq. (5) can be simplified as

$$S_{n^+-n} = \frac{D_p^+ N_D^- n_{ie}^2}{W_n^+ N_D^+ n_D^2}. \quad (6)$$

Detailed band structure calculations by Bennett and Lowney¹⁰ show that n_{ie} is much greater than n_D due to strong effective band-gap shrinkage in p^+ -GaAs, but for n^+ -GaAs, majority-carrier degeneracy acts to reduce n_{ie} and should offset band-gap shrinkage effects. This implies that the strong increase in n_{ie} observed in p^+ -GaAs is absent in n^+ -GaAs. For very heavy n -type doping, n_{ie} may actually be less than n_D .

Theoretical estimates of S_{n^+-n} with and without heavy doping effects were calculated for a range of heavy doping concentrations, N_D^+ , using Eq. (6) with the same W_n^+ and N_D^- from our device. For heavy doping effects, we used the theoretical calculations (n_{ie}^2/n_D^2) of Bennett and Lowney.¹⁰ In the absence of heavy doping effects, (n_{ie}^2/n_D^2) is set to be one. The experimental values for majority-carrier hole mobility from Sze⁸ were used to deduce D_p^+ . Figure 8 shows the theoretical estimates of S_{n^+-n} with and without heavy doping effects versus N_D^+ . As expected, heavy doping effects have only a minor effect on the results. However, the improving characteristics for $N_D^+ > 2 \times 10^{18}$ cm^{-3} are attributed to an effective widening of the band gap caused by majority-carrier degeneracy. Note that at $N_D^+ = 3 \times 10^{18}$ cm^{-3} , the theoretical value of S_{n^+-n} is approximately equal to 650 cm/s. This is consistent with our experimental estimate that S_{n^+-n} is less than 1×10^3 cm/s, and with that recently reported for Si-doped, n^+-n GaAs homojunction barriers grown by MOCVD.⁷

V. CONCLUSIONS

In this paper, the electrical performance of Si-doped n^+-n GaAs homojunction barriers grown by MBE is characterized and analyzed. We employed a successive etch technique to study hole injection currents in GaAs n^+-n-p^+ solar cells. The results of the analysis show that minority-carrier holes in our MBE-grown material have a mobility of 293 $\text{cm}^2/\text{V s}$ for an n -type Si-doping level of 1.5×10^{16} cm^{-3} at 300 K. The interface recombination velocity for these n^+-n GaAs homojunction barriers is estimated to be less than 1×10^3 cm/s, and it appears to be comparable to that recently observed for Si-doped, n^+-n GaAs homojunction barriers grown by MOCVD.⁷ We present evidence that these n^+-n GaAs homojunctions, unlike the p^+-p GaAs homojunctions, are almost as effective as AlGaAs heterojunctions in

minority-carrier confinement, and that their electrical performance is not degraded by heavy doping effects. This work helps to explain the superior performance of a $p^+ - n$ solar cell with an $n^+ - n$ back-surface field compared to an $n^+ - p$ solar cell with a $p^+ - p$ back-surface field.

ACKNOWLEDGMENTS

This work was supported by the Solar Energy Research Institute under Subcontract No. XL-5-05018-1. H. L. Chuang and M. E. Klausmeier-Brown were supported by the Indiana Corporation for Science and Technology, and the Eastman-Kodak Company, respectively.

¹S. P. Tobin, C. Bajgar, S. M. Vernon, L. M. Goeffroy, C. J. Keavney, M. M. Sanfacion, V. E. Haven, M. B. Spitzer, and K. A. Emery, Proceedings

of the 19th IEEE Photovoltaic Specialists Conference, May 4-8, 1987, p. 1492.

²H. F. MacMillan, N. R. Kaminar, M. S. Kuryla, M. J. Ladle, D. D. Liu, G. F. Virshup, J. M. Gee, in Proceedings of the 20th IEEE Photovoltaic Specialists Conference (IEEE, New York, 1988) (to be published).

³H. L. Chuang, P. D. DeMoulin, M. E. Klausmeier-Brown, M. R. Melloch, and M. S. Lundstrom, *J. Appl. Phys.* **64**, 6361 (1988).

⁴M. E. Klausmeier-Brown, C. S. Kyono, P. D. DeMoulin, S. P. Tobin, M. S. Lundstrom, and M. R. Melloch, *IEEE Trans. Electron Devices* **ED-35**, 1159 (1988).

⁵R. P. Leon, Conference Recordings of the 19th IEEE Photovoltaic Specialists Conference, May 4-8, 1987, p. 808.

⁶J. S. Blakemore, *J. Appl. Phys.* **53**, R123 (1982).

⁷R. Venkatsubramanian, S. Bothra, S. K. Ghandhi, and J. M. Borrego, to be published in Proceedings of the 20th IEEE Photovoltaic Specialists Conference (IEEE, New York, 1988).

⁸S. M. Sze, *Physics of Semiconductor Devices*, 2nd ed. (Wiley, New York, 1981).

⁹P. D. DeMoulin, M. S. Lundstrom, and R. J. Schwartz, *Solar Cells* **20**, 229 (1987).

¹⁰H. S. Bennett and J. R. Lowney, *J. Appl. Phys.* **62**, 521 (1987).